Aerosol and Air Quality Research, 19: 1056–1067, 2019

ISSN: 1680-8584 print / 2071-1409 online
doi: 10.4209/aaqr.2018.09.0351

Three-year Long Source Apportionment Study of Airborne Particles in Ulaanbaatar Using X-ray Fluorescence and Positive Matrix Factorization

Gerelmaa Gunchin[1,2*], Manousos Manousakas[3], Janos Osan[2,4], Andreas Germanos Karydas[5], Konstantinos Eleftheriadis[3], Sereeter Lodoysamba[6], Dagva Shagjjamba[1], Alessandro Migliori[2], Roman Padilla-Alvarez[2], Christina Streli[7], Iain Darby[2,8]

[1] *Nuclear Research Center, National University of Mongolia, Ulaanbaatar, Mongolia*
[2] *Nuclear Science and Instrumentation Laboratory, Physics section, IAEA, Seibersdorf, Austria*
[3] *Institute of Nuclear & Radiological Sciences & Technology, Energy & Safety, N.C.S.R. Demokritos, Greece*
[4] *Environmental Physics Department, Hungarian Academy of Sciences Centre for Energy Research, Budapest, Hungary*
[5] *Institute of Nuclear and Particle Physics, N.C.S.R "Demokritos", Athens, Greece*
[6] *Faculty of Engineering, German-Mongolian Institute for Resources and Technology, Ulaanbaatar, Mongolia*
[7] *Vienna University of Technology, Atominstitut, Vienna, Austria*
[8] *SUPA, School of Physics and Astronomy, University of Glasgow, Glasgow, United Kingdom*

ABSTRACT

The capital city of Mongolia, Ulaanbaatar, suffers from high levels of pollution due to excessive airborne particulate matter (APM). A lack of systematic data for the region has inspired investigation into the type, origin and seasonal variations of this pollution, the effects of meteorological conditions and even the time-dependence of anthropogenic sources. This work reports source apportionment results from a large data set of 184 samples each of fine ($PM_{2.5}$) and coarse ($PM_{2.5-10}$) fraction atmospheric PM collected over a three-year period (2014–2016) in Ulaanbaatar, Mongolia. Positive Matrix Factorization (PMF) was applied using the concentrations of 16 elements measured by an energy dispersive X-ray fluorescence spectrometer along with the black carbon content measured by a reflectometer as input data. The PMF results revealed that whereas mixed sources dominate the coarse fraction, soil and traffic sources are the principle contributors to the fine fraction. The source profiles and the seasonal variations of their contributions indicate that fly ash emanating from coal combustion mixes with traffic emissions and resuspended soil, resulting in variable chemical source profiles. Four sources were identified for both fractions, namely, soil, coal combustion, traffic and oil combustion, which respectively contributed 35%, 16%, 41% and 8% to the coarse fraction and 31%, 27%, 31% and 11% to the fine fraction. Additionally, the probable source contributions from long-range transport events were assessed via concentration-weighted trajectory analysis.

Keywords: Airborne particulate matter; XRF; PMF; Ulaanbaatar.

INTRODUCTION

Atmospheric pollution due to particulate matter (PM) is a wide concern for both human health and the climate (Cohen *et al.*, 2004; Ostro *et al.*, 2015). Aerosol particles can be formed either from precursor gases via chemical reactions in the atmosphere or be directly emitted from various sources of anthropogenic and natural origin (Davy *et al.*, 2011). PM is a mixture of organic and inorganic compounds and it is important to be able to identify its sources and quantify their contributions (Hasenkopf *et al.*, 2016; Diapouli *et al.*, 2017).

The process of identification and apportionment of pollutants to their sources is an important step in air quality management, since this can be used as baseline data for the establishment of air pollution mitigation strategies. Multivariate receptor models are very useful tools as they may be applied directly to the observed PM composition data (Santoso *et al.*, 2008). The dataset of the PM elemental composition is an essential input for the characterization of specific emission sources using statistical apportionment tools such as the Positive Matrix Factorization (PMF) model (Paatero *et al.*, 2003), and can be accompanied by complementary data (e.g., black carbon, organic carbon, water-soluble ions). Generally, major

* Corresponding author.
E-mail address: gerelmaa-g@num.edu.mn

elements such as Mg, Al, Si, Ca, Ti and Fe are primarily associated with windblown soil, S with fossil fuel burning, and K with smoke and biomass burning, whereas Cr, Mn, Fe, Cu and Zn are associated with industrial processes, while Pb and Br derive from motor vehicle exhaust (Cohen *et al.*, 2014; Manousakas *et al.*, 2015). For a comprehensive source apportionment, a group of analytical techniques should be applied to determine the concentration of the maximum number of elements being either major, minor or trace constituents of the PM mass. Importantly, the respective uncertainties for the elemental concentrations should be well defined for source apportionment studies, as they are used in the model.

X-ray fluorescence (XRF) analysis is a multi-elemental, sensitive and very versatile analytical method widely used in various scientific fields and amongst the ones best suited for environmental researches and particularly for PM analyses (Calzolai *et al.*, 2008; Shaltout *et al.*, 2017; Prost *et al.*, 2018). In this study, an energy-dispersive XRF spectrometer (Epsilon 5; PANalytical, Inc., Almelo, the Netherlands) was used for the elemental analysis. The combined result of employing several secondary targets, coupled within a three-dimensional polarizing optical geometry, leads to the significant reduction in the measured PM XRF spectrum of the scattered X-rays from the tube emission, thus lowering the continuum counts (noise signal). Such a reduction of the noise signal, in combination with the instrument sensitivity gains achieved by optimizing the excitation conditions for different groups of elements, enables obtaining minimum detection limits in the low ng cm^{-2} range or even below for most of the elements of interest (Shaltout *et al.*, 2018). For the determination of black carbon (BC) content, an M43D smoke stain reflectometer from Diffusion Systems Ltd. (London, United Kingdom) was used.

Herein we present source apportionment results from a large data set of fine ($PM_{2.5}$) and coarse ($PM_{2.5\text{-}10}$) fraction atmospheric PM samples collected over a three-year period (2014–2016) in Ulaanbaatar, Mongolia.

METHODS

Sample Collection

Mongolia is located across northeast and central Asia at an average altitude of 1400 m above sea level. Its elevation, relatively high latitude, non-coastal geography and the effects of Siberian anticyclone weather patterns give the country a continental dry climate with long, cold winters and relatively short summers. Average temperatures from November to March drop below 0°C over the whole country. The capital and largest city, Ulaanbaatar, is located on Tuul River Valley and surrounded by mountains. The total area of the city is 4735.1 km^2 and has approximately 1.4 million inhabitants, comprising 45% of the whole country's population. According to a recent report (Ulaanbaatar City Governor's Implementation Agency, 2016), 43.3% of Ulaanbaatar residents live in apartment buildings which are connected to the main central heating grid and the remaining 56.7% of inhabitants live in traditional Mongolian dwelling areas, called *ger khoroolol*, where coal, wood and other household materials are used as fuel for domestic heating and cooking purposes. The annual consumption statistics of coal and wood for Ulaanbaatar inhabitants are described elsewhere (Guttikunda, 2007). The regional climate, geographical location and residential features of Ulaanbaatar city intensify a winter air pollution problem. It is for these reasons that Ulaanbaatar is reported as one of the world's most polluted cities (World Bank, 2011).

A total of 184 air particulate matter samples, size-fractionated according to aerodynamic diameter between 10 microns and 2.5 microns ($PM_{10–2.5}$, or coarse fraction) and 2.5 microns or less ($PM_{2.5}$, or fine fraction), were collected for two days per week (Monday and Thursday) throughout the period 2014–2016. The sampling site was located at the Nuclear Research Center (NRC) of the National University of Mongolia (NUM) (Fig. 1). The monitoring site is surrounded by a combination of buildings, *ger khoroolol*, paved and unpaved roads.

Sampling was undertaken using a GENT instrument (Maenhaut *et al.*, 1993), comprising a PM_{10} impactor-type size-selective inlet and a stacked filter unit (SFU) assembly connected to a pump and an air flow meter. The SFU is made up of two filters arranged sequentially. The upper filter (with 8-μm pore size, type polycarbonate) collects the coarse fraction, and the lower filter (with 0.4-μm pore size, type polycarbonate) collects the fine fraction. The average air flow rate was 16.0 L min^{-1} and the average mass loadings for $PM_{2.5}$ and $PM_{10\text{-}2.5}$ were 92 μg m^{-3} and 131 μg m^{-3}, respectively. The collection of the samples covered a 24-hour period. However, on winter days it was not possible to collect over the entire 24 hours as high pollution resulted in clogging of the filters. Therefore, the sampler was operated during alternating on and off periods over the course of the 24 hours so as to provide a representative sample for that day.

Gravimetric masses of the samples were obtained in triplicate measurements using a digital weighing balance that has an automatic calibration function to ensure accuracy. Gravimetric masses were subsequently divided by the sampled air volume to calculate average PM mass concentrations.

The black carbon (BC) measurement and its quantification model are described elsewhere (Davy *et al.*, 2011).

Elemental Analysis, XRF

XRF analysis has been performed in the IAEA Nuclear Science and Instrumentation Laboratory (NSIL) in Seibersdorf, Austria. The spectrometer features a variety of secondary targets, such as Al, CaF_2, Fe, Ge, Zr, Mo, Ag and Al_2O_3 (Barkla polarization target) which are excited by an Sc-W tube. The characteristic X-ray radiation emitted by the sample is detected by a Ge detector with a measured energy resolution of approximately 150 eV FWHM at Mn-Kα (5.89 keV). Eight measuring conditions were selected to optimize the analytical sensitivity and precision for the determination of certain groups of elements in aerosol particles on filters as presented in Table 1. For all secondary and polarization targets, the live time of the measurements was set to 300 seconds. The analysis was performed in vacuum.

Fig. 1. Nuclear Research Center (NRC) air quality monitoring site, 4 kilometers east of the center of Ulaanbaatar (latitude: 47°55′, longitude: 106°55′, 1300 m above sea level). Source: ©1992 MAGELLAN Geographix™ and https://maps.google.com/.

Table 1. XRF spectrometer (PANalytical Epsilon 5) conditions for elemental analysis of APM.

Nr.	Targets	Detected elements	Voltage (kV)	Current (mA)
1	Al	(Na), Mg	25	24
2	CaF_2	Al, Si, P, S, Cl, K	40	15
3	Fe	Ca, Sc, Ti, V, Cr	75	8
4	Ge	Mn, Fe, Co, Ni, Cu, Zn	75	8
5	Zr	Ga, Ge, As, Se, Br, Pb-L	100	6
6	Mo	Sr, Y	100	6
7	Ag	Zr, Nb, Mo, Tc, Ru	100	6
8	Al_2O_3	Rh, Pd, Ag, Cd, In, Sn, Sb, Te, I, Cs, Ba, La, Ce	100	6

The quantification was based on a calibration performed by measuring thin film single element and compound reference materials (Micromatter, Surrey, BC, Canada), prepared on a polycarbonate filter support. The nominal areal densities of the certified materials ranged between 43.8 μg cm^{-2} and 62.3 μg cm^{-2} with relative uncertainties quoted as 5%. The following standards were used for calibration purposes: NaCl, MgF_2, Al, SiO, KCl, CaF_2, Ti, V, Mn, Fe, Co, Ni, Cu, ZnTe, Nb_2O_3, MoO_3, CdSe, Sn, Sb, BaF_2, CeF_3, NdF_3, HoF_3, YbF_3, WO_3, Au, TlCl and Pb. A Standard Reference Material of particulate matter on filter media (SRM 2783; NIST, Gaithersburg, MD, USA) was used for validation of the analytical method. The provided software of the Epsilon 5 was used for spectrum deconvolution, whereas the elemental concentrations were calculated using a sensitivity curve determined by the available set of thin single- or two-element standards.

For the estimation of the combined uncertainty of the results, the following contributing factors were considered: the peak area statistical uncertainty, the fitting error in the calibration (sensitivity) curve, the quoted uncertainties of the elemental areal densities reported for the standards (5%), the estimated error due to the omittance of the self-attenuation effect for the excitation and detection of light-element characteristic X-rays (the calibration was based on presuming the samples as infinitely thin in the sense of X-ray attenuation), as well as the relative standard deviation of three replicate measurements (reproducibility in operation). The self-attenuation effect occurs significantly within the PM sample components due to the low energy of the exciting and characteristic X-rays used in the measurement of light elements. According to a previous study (Gutknecht *et al.*, 2010), the bias of results due to the omittance of self-attenuation correction is estimated to be 16% for Na, 12% for Mg and 11% for Al and Si, whereas for the rest of measured elements is considered as 1%. The measurement's precision was calculated as the standard deviation of results from three consecutive measurements for twenty representative samples. Finally, the combined relative uncertainty is calculated as the square root of the sum of squares of the various contributing relative uncertainties (Gutknecht *et al.*, 2010; Manousakas *et al.*, 2017).

The elemental minimum detection limits (MDLs) were obtained by measuring the National Institute for Standards and Technology (NIST) Standard Reference Material (SRM) 2783. In Fig. 2, the MDLs of the measured elements are presented for a measurement time of 300 s and the employed secondary target for each element is denoted by

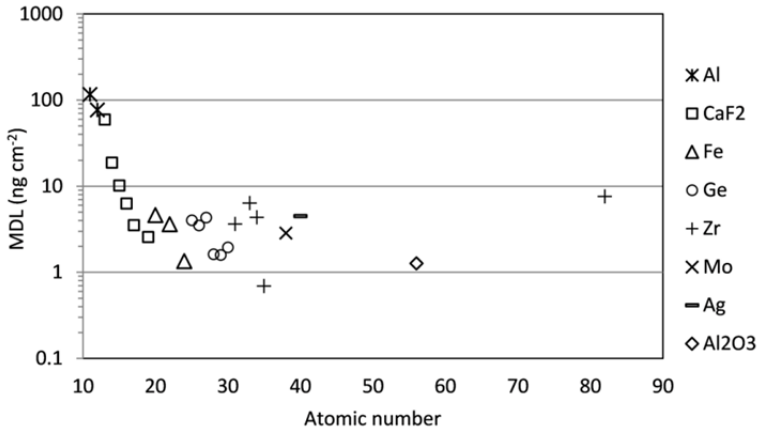

Fig. 2. Minimum detection limit values established from the NIST reference material (SRM 2783) air particulate filter.

different symbols. The detection limits were calculated taking three times the square root of background counts (measured continuum under the characteristic peak) as the minimum detectable peak area.

Positive Matrix Factorization

U.S. EPA Positive Matrix Factorization (PMF) (Paatero, 1997) 5.0 was used for the source identification and apportionment of both the $PM_{2.5}$ and $PM_{10\text{-}2.5}$ fractions. Fifteen species of $PM_{10\text{-}2.5}$ (BC, Na, Mg, Al, Si, S, Cl, K, Ca, Ti, Mn, Fe, Zn, Pb and Mass) and twelve species of $PM_{2.5}$ (BC, Al, Si, S, K, Ca, Ti, Mn, Fe, Zn, Pb and Mass) were used for the PMF modeling. Na, Mg, and Cl were considered as "weak" or "bad" depending on the uncertainties that were associated with their measurement.

The basic equation that refers to the solution of the mass balance problem is common for all receptor models including PMF. The equation can be written as Eq. (1):

$$X = G \times F + E \quad (1)$$

where X is the concentration of species measured on sample, G is the contribution of the source, F the source profile and E the residual. Since the PMF solution is not unique, to obtain the optimum solution G and F are adjusted until a minimum Q for a given number of factors is found. Q is defined as Eq. (2):

$$Q = \sum_{j=1}^{m} \sum_{i=1}^{n} \frac{E_{ij}^2}{S_{ij}^2} \quad (2)$$

where s_{ij} is the uncertainty of the j^{th} species concentration in sample i, n is the number of samples, and m is the number of species.

Solutions with a number of factors from 3 to 8 were investigated in order to identify the meaningful solution with the highest number of factors. For both PM fractions the optimum solution was found to be for 4 factors. Data were screened by their uncertainties (signal-to-noise ratio (S/N) in PMF). Variables with very low S/N ratios (≤ 0.2) were defined to be bad and excluded from the analysis, while weak variables ($0.2 \leq S/N \leq 2$) were down-weighted (Paatero and Hopke, 2003). For $PM_{2.5}$ analysis, the elements Na, Mg and Cl were excluded; V and Cr were defined as "bad" and BC, Cu, Zn, Pb and As were defined as "weak" variables and for $PM_{10\text{-}2.5}$ analysis only Cr was defined as "bad" and BC, Na, Mg, Cl, Ni, Zn, Pb and As species were defined as "weak". The mass was set as total variable for analyses. The robustness of the solutions was investigated using the uncertainty estimation tool that EPA PMF 5.0 offers. According to bootstrap analysis (Reff *et al.*, 2007) the factors were reproduced at a level higher that 80%, while no factor swaps appeared for the minimum level of Q at displacement and bootstrap displacement analysis. The comparison between predicted (PMF) and gravimetric masses of both the fractions were found to be high ($R^2_{coarse} = 0.82$ and $R^2_{fine} = 0.86$).

RESULTS

Particulate Matter Concentrations

The average concentrations of annual and seasonal coarse and fine particulates are shown in Tables 2 and 4. The presented values indicated that annual concentrations of both the fractions are much higher than Mongolian National Ambient Air Quality Standards (MNS 4585:2007), set to yearly averages of 50 μg m^{-3} for PM_{10} and 25 μg m^{-3} for $PM_{2.5}$, as well as the World Health Organization (WHO)'s guideline (WHO, 2005) corresponding values of 20 μg m^{-3} and 10 μg m^{-3}. PM_{10} limit values are used in the text not for direct comparison but as reference to provide a better metric regarding the measured mass concentration levels. Particulate matter concentrations were dominated by the coarse fraction for the whole study period. The maximum concentrations were measured at 580 μg m^{-3} for the coarse particle and 7% of the total sampling days were above 300 μg m^{-3}, and the annual and seasonal values show that no drastic difference between warm (April–September) and cold (October–March) season averages exist (Fig. 3). The fine particle concentration increases during the cold season and highest values were recorded during winter months while the concentration went often over 100 μg m^{-3}.

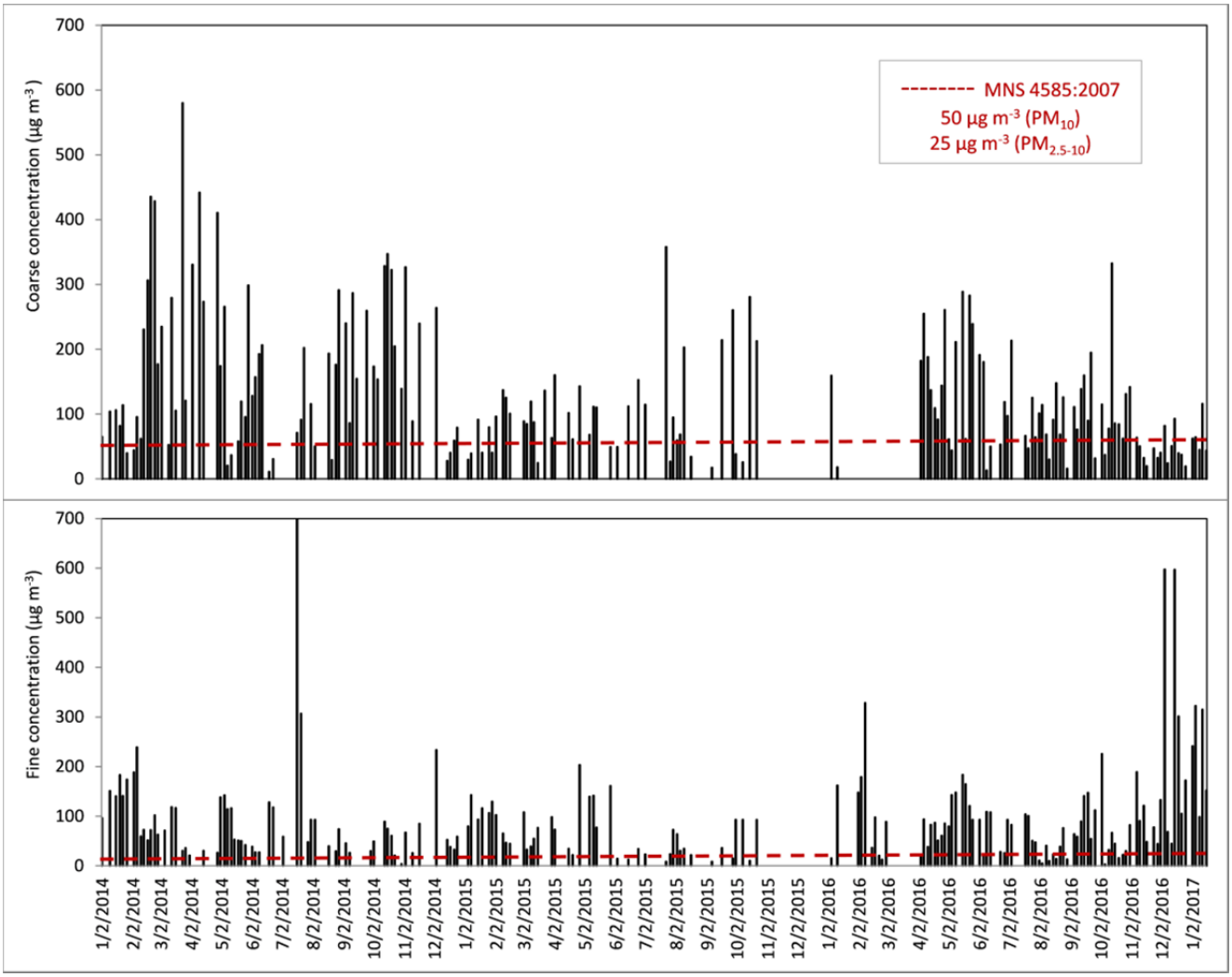

Fig. 3. Time series of both $PM_{10\text{-}2.5}$ (upper) and $PM_{2.5}$ (lower) fractions at the sampling site, from January 2014 to January 2017.

PMF Analysis Results

$PM_{10\text{-}2.5}$ Data Analysis

In Table 2, the descriptive statistics regarding $PM_{10\text{-}2.5}$ and elemental mass concentrations are presented. The minimum detection limits (MDLs), number of elemental constituents which were detected above their respective MDLs, as well as average elemental concentrations during warm and cold season are also included in the table.

As presented in Table 2, for the coarse fraction the elements Al, Si, Ca, Ti and Fe originate mainly from a crustal matter source and were higher in the warm period. The Si:Al ratio was found to be 2.6, indicative of a typical soil composition—aluminosilicates (Lide, 1992).

Several Factors (3–8) were used in order to obtain the optimum PMF solution, and settling upon 4 contributing factors to be the solution was chosen with regard to the highest number of factors with physical sense. The factors have been identified based on the key elements in the source fingerprint and the correlations between them. The selected sources are traffic, soil, coal combustion and oil and their elemental profiles are presented in Fig. 4.

The first profile has been identified as traffic, although elemental profile shows that this factor can be a combination of several combustion sources as it contains the highest percentage of BC and S, as well as elements with crustal and anthropogenic origin. However, the high percentage of elements such as Ni, Cu, Zn and Pb indicates that this factor mainly represents a traffic source (Sarigiannis *et al.*, 2017). This source contributes 41% of the total $PM_{10\text{-}2.5}$ mass and seasonal variation presents higher contribution in the cold season. The fact that the source has higher contribution during the cold season is another indication that the source is mixed with other combustion sources such as coal, which is used for residential heating and is expected to have a higher contribution during the cold season.

The second source profile was identified as soil since it contains crustal matter elements Mg, Al, Si, Ca, Ti, Mn and Fe. Moreover, this factor has high presence of Na, Cl, K and Zn which indicates that it might be mixed with some other sources such as salt and anthropogenic sources that can contribute to this source by soil resuspension (Eleftheriadis and Colbeck, 2001). The contribution of this source is 35%

Table 2. Summary statistics for $PM_{10-2.5}$, BC and elemental concentrations.

ng m^{-3}	Average	S.D	Median	Max.	Min.	# Samples > MDL	Warm	Cold
Mass	131000	102000	101000	579000	10800	183	136000	123000
BC	3850	2130	3800	11300	372	182	3430	4870
Na	708	394	625	3260	142	183	689	750
Mg	604	325	549	1770	126	176	616	592
Al	4660	3400	4000	15000	376	183	5140	4030
Si	12500	9340	10900	40700	855	183	13900	10600
S	1000	913	662	4560	57.0	183	708	1600
Cl	338	280	266	1960	34.0	183	334	327
K	1830	1390	1550	6170	124	183	2040	1540
Ca	4270	2800	3580	15000	494	183	4510	3910
Ti	368	264	322	1190	32.0	183	406	314
V	5.00	4.00	4.00	17.0	5.00	161	5.00	4.00
Cr	7.00	4.00	7.00	23.0	2.00	183	7.00	8.00
Mn	99.0	67.0	84.0	318	10.0	183	107	91.0
Fe	3930	2840	3250	13200	316	183	4280	3450
Ni	4.00	2.00	4.00	16.0	2.00	182	4.00	4.00
Cu	18.0	9.0	16.0	74.0	5.00	183	17.0	19.0
Zn	62.0	46.0	52.0	271	5.00	183	60.0	69.0
Pb	29.0	28.0	23.0	316	8.00	183	24.0	37.0
As	8.00	8.00	6.00	46.0	6.00	130	7.00	11.0

of the total $PM_{10-2.5}$ mass. Seasonal variations indicated that this source has a higher contribution during the warm period (Fig. 5).

The third source profile, coal combustion, is traced by the high concentration of BC and S. It is not very common that a combustion source affects the coarse PM fraction to that extent. A possible explanation for this can be that as the ashes which remain in the stove after the burning of coal for domestic heating are in many cases discarded by the populace on the soil, the ashes may then become resuspended along with soil and other anthropogenic related elements. The contribution of this source is 16%.

The last factor was identified as oil combustion as it contains a significant amount of V and Ni. Interestingly, this source is for the first time identified on this site. In previous studies conducted in the area (Davy *et al.*, 2011; Gunchin *et al.*, 2012) this source profile was not found. This source has a contribution of 8% of the total mass and presents low temporal variation.

The output of PMF was used to calculate the annual contribution of the sources for the three years of the study. Table 3 presents average mass contributions of the sources to the $PM_{10-2.5}$ fraction for each year. The results of Table 3 reveal that the sources of the coarse fraction appear to be stable for the three years of the study period. However, the average mass of the year 2015 was relatively low when compared with that of the years 2014 and 2016. This might be affected by the missing data of November and December 2015. As it is presented in Table 3, the variance in the source contributions for the three years the study was conducted is low.

$PM_{2.5}$ Data Analysis

Table 4 presents $PM_{2.5}$ descriptive statistics. The minimum detection limits (MDLs), number of elemental constituents which were detected above their respective MDLs and average concentrations during warm and cold season are also included in Table 4. As presented in Table 4, BC, S, Zn and As species significantly dominate the fine fraction. The average concentrations were much higher in cold periods compared to warm seasons. The correlation of BC and S components was 0.96, clearly indicating that they have a common source which is likely coal combustion.

Based on the key contribution of certain elements, the number of sources that were identified for the fine fraction was 4 as well. These are soil, traffic, coal combustion and oil. The elemental source profiles are presented in Fig. 6.

The elemental profile of soil includes clear contribution of crustal matter elements such as Mg, Al, Si, Ca, Ti, Mn and Fe. The correlation of the concentrations of Al and Si was 0.96 which indicates typical soil origin. The contribution of this source is 31% of the total $PM_{2.5}$ mass and it is slightly higher during the warm period than the annual average (Fig. 7).

The second source profile is identified as traffic. Higher percentage of elements such as Ni, Cu, Zn and Pb in this profile indicates that this factor mainly from traffic. This source has a contribution of 31% of the total $PM_{2.5}$ mass. However, this source profile also includes a high presence of BC and this might influence the total contribution of this source. Seasonal variance shows this factor has higher contribution during the cold season.

The third source has been identified as coal combustion since it is characterized by significantly higher concentrations of BC and S. The correlation of these two components was 0.90. This factor represented 27% of the total $PM_{2.5}$ mass. Interestingly, contribution of this source was lower than crustal matter source in a fine fraction. However, this factor also containing different source elements such as V, Zn and Pb which indicates that the factors is slightly mixed

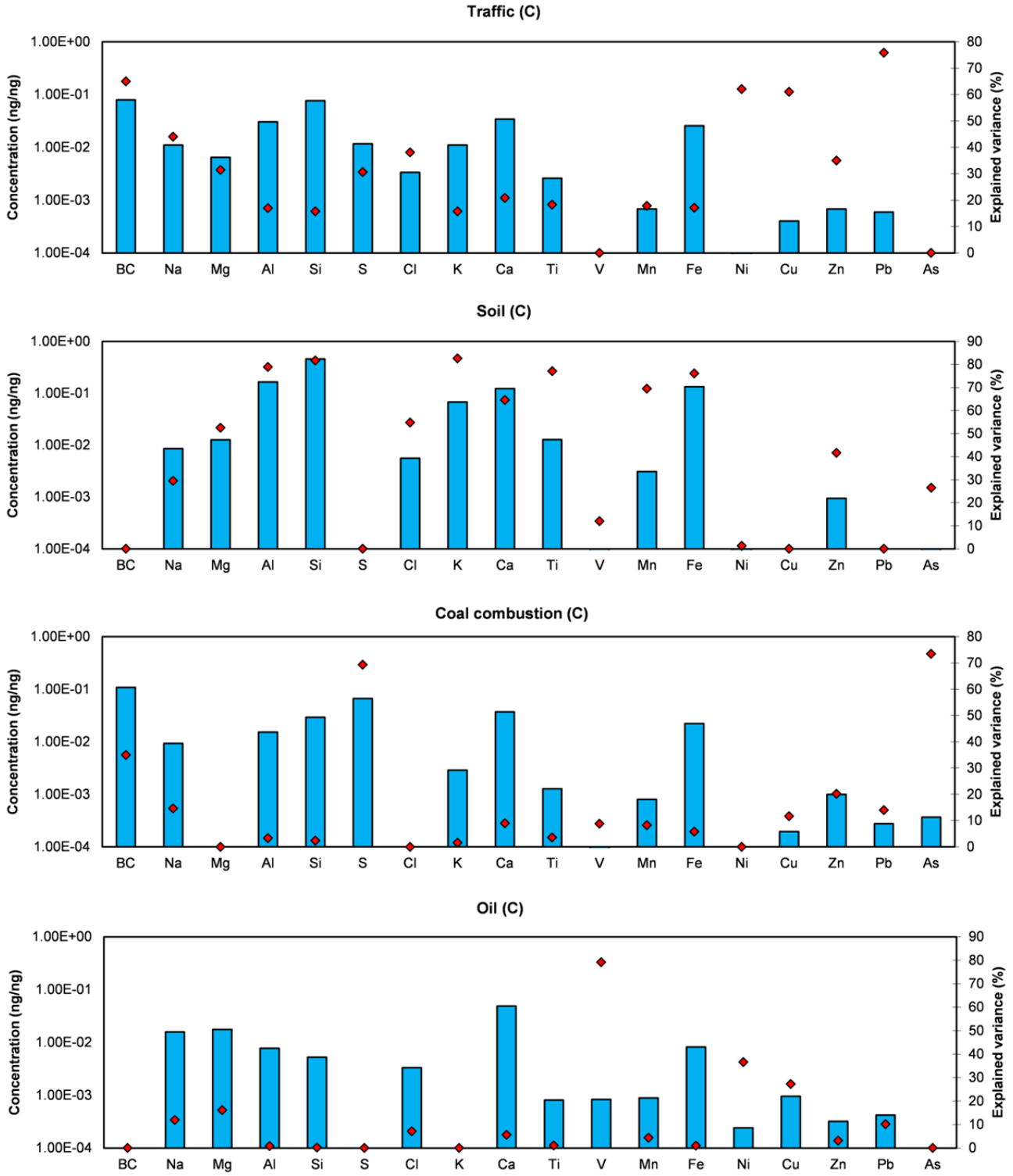

Fig. 4. Elemental source profiles derived by PMF for $PM_{10-2.5}$ samples.

with traffic and road dust. Additionally, As appears in this source profile in relatively enhanced concentration. The same feature applies to coal combustion source in the coarse fraction as well. It should be noted that As is a known tracer of coal combustion.

The last factor identified as oil presents the very similar source profile as the coarse fraction, and has a significant amount of V and Ni. A contribution of this source has 11% of the total mass and has higher seasonal trend during the cold months.

The annual contributions were calculated for the fine fraction as well. Table 5 presents average mass contributions of each year of the $PM_{2.5}$ sources. It seems that in 2016 the coal combustion source was increased by 13–15%, whereas

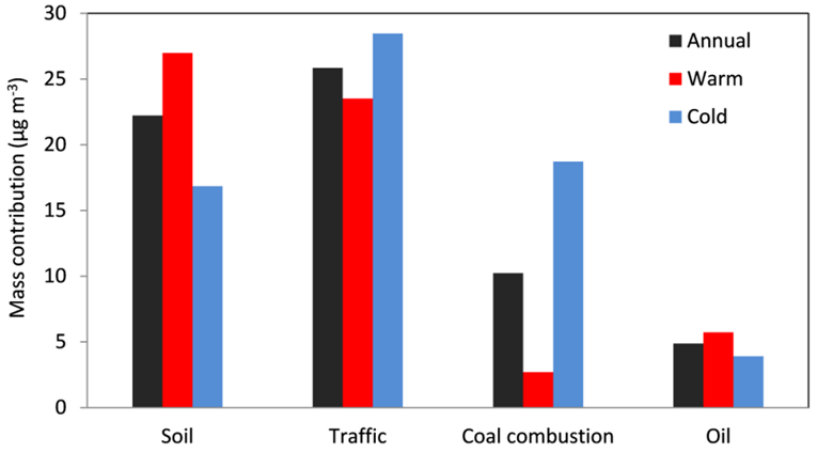

Fig. 5. Seasonal source mass contribution to $PM_{10\text{-}2.5}$.

Table 3. Yearly source contributions to $PM_{10\text{-}2.5}$.

Sources	2014		2015		2016	
	Average (μg m^{-3})	%	Average (μg m^{-3})	%	Average (μg m^{-3})	%
Traffic	28	42	14	37	25	43
Soil	24	36	12	39	19	32
Coal combustion	10	15	5	17	10	17
Oil	5	8	3	8	5	8

Table 4. Summary statistics for $PM_{2.5}$, BC and elemental concentrations.

ng m^{-3}	Average	S.D	Median	Max.	Min.	# Samples > MDL	Warm	Cold
Mass	92800	95200	72700	70000	2770	184	77300	10800
BC	6590	6340	4260	50900	1030	184	3120	10100
Na	391	210	331	1900	69.0	184	304	478
Mg	251	178	218	1600	91.0	157	210	299
Al	737	470	588	2292	133	184	739	736
Si	1490	1110	1130	5570	141	184	1550	1430
S	1740	2600	684	20600	119	184	458	30490
Cl	43.0	69.0	28.0	817	5.00	182	30.0	56.0
K	259	155	214	946	23	184	241	276
Ca	567	390	449	2690	50.0	184	511	626
Ti	38.0	28.0	30.0	153	4.00	184	40.0	37.0
V	2.00	1.00	2.00	6.00	2.00	70	2.00	3.00
Cr	5.00	5.00	4.00	37.0	2.00	173	3.00	6.00
Mn	18.0	10.0	15.0	51.0	4.0	183	16.0	21.0
Fe	455	312	350	1950	34.0	184	431	479
Ni	3.00	1.00	2.00	8.00	2.00	128	2.00	3.00
Cu	5.00	10.0	3.00	126	2.00	166	5.00	6.00
Zn	45.0	41.0	30.0	260	2.00	184	29.0	61.0
As	28.0	38.0	18.0	394	7.00	183	15.0	42.0
Pb	11.0	9.00	8.00	53.0	5.00	87	5.00	12.0

oppositely the soil source was decreased. The traffic source was higher in 2014 and during the next two years it was quite constant. The oil source was also relatively stable during the period of study.

Concentration Weighted Trajectory Analysis

The concentration weighted trajectory (CWT) is a type of statistical trajectory model and it is widely used to locate the regional source areas potentially affecting the receptor site by long-range transportation (Chandra *et al.*, 2014). In this method, the mean concentration is calculated and used as weight for the residence time of the trajectory in each modeled grid cell and assigned equally to all segments of trajectory (Wang *et al.*, 2009). Back trajectory calculations were done by HYSPLIT (Hybrid Single-Particle Lagrangian Integrated Trajectory) model using a global

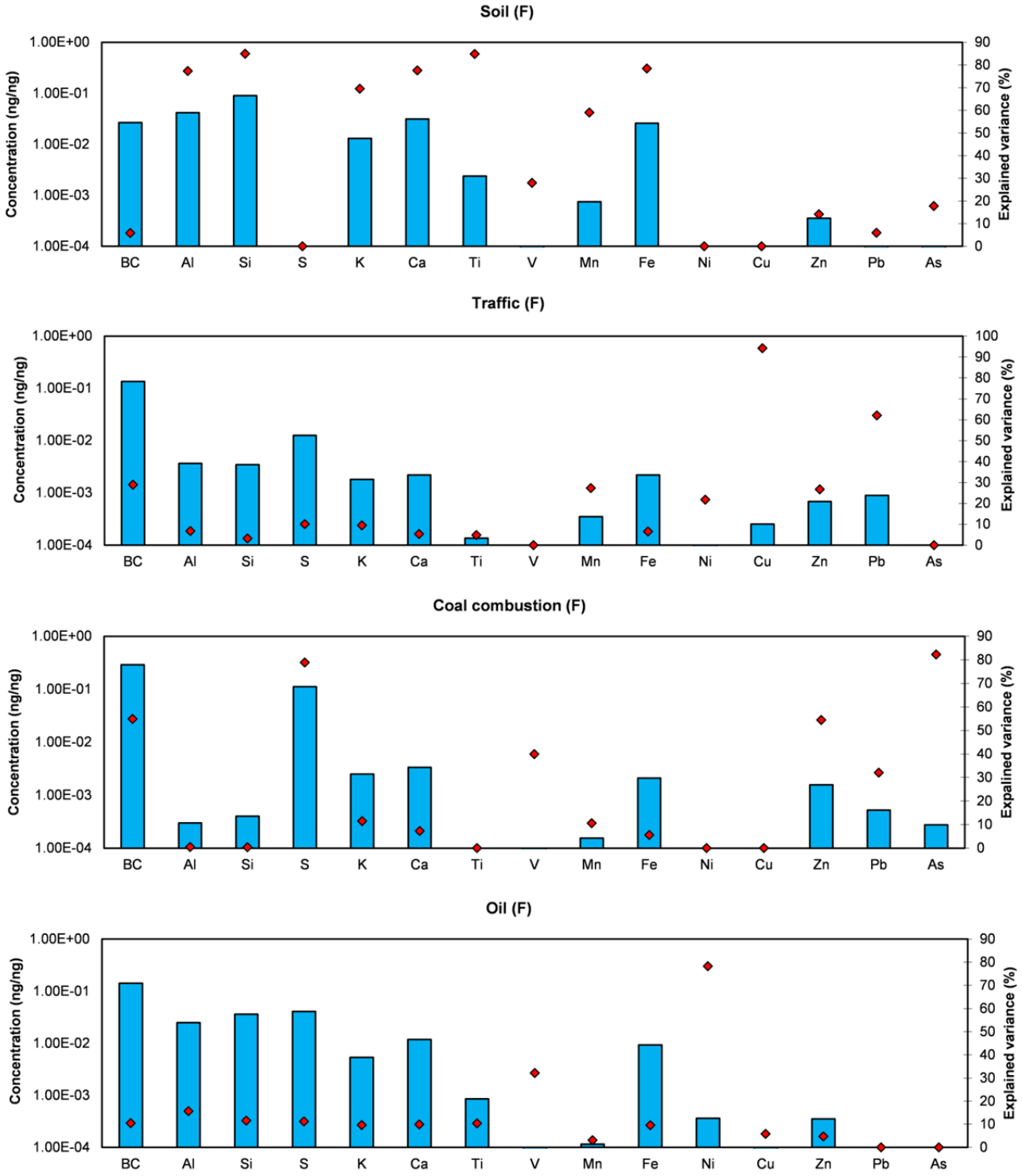

Fig. 6. Elemental source profiles derived by PMF for $PM_{2.5}$ samples.

meteorological dataset GDAS. The trajectories were computed for an altitude of 1500 m above ground level and 120 hours backward for the sampling days. The height was selected to better represent long-range transport events. Otherwise, it may be affected by local sources and topography. For the CWTs, Zefir tool was used (Petit *et al.*, 2016).

Fig. 8 shows air mass back trajectories of each source of $PM_{2.5}$ contributions. From the result of the CWT analyses, it seems clear that northwest and north part contributes dominantly to the sampling area. Due to the breakdown in Siberian high-pressure zone, wind originates usually from northwest direction to Ulaanbaatar (Davy *et al.*, 2011). However, the combustion and traffic source trajectories indicate a more local behavior. The oil source seems affected from long-range transportation from northerly direction.

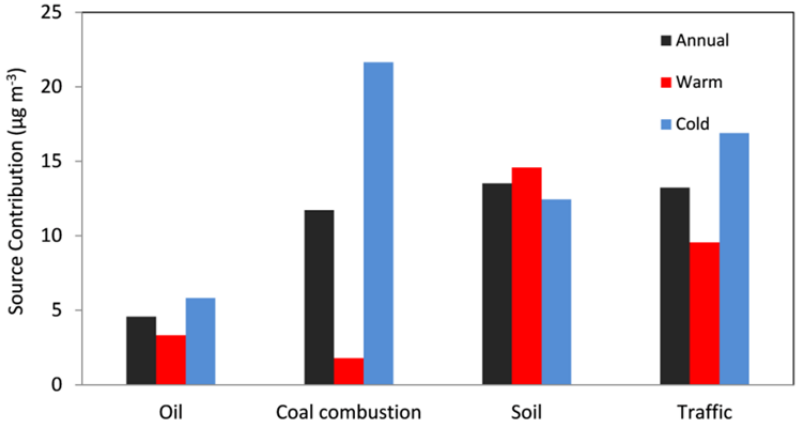

Fig. 7. Seasonal source mass contribution to $PM_{2.5}$.

Table 5. Yearly source contributions to $PM_{2.5}$ by average mass and percentage.

Sources	2014		2015		2016	
	Average (μg m^{-3})	%	Average (μg m^{-3})	%	Average (μg m^{-3})	%
Soil	12	31	16	40	14	28
Traffic	14	36	11	28	14	29
Coal combustion	8	21	8	19	17	34
Oil	4	12	5	14	4	9

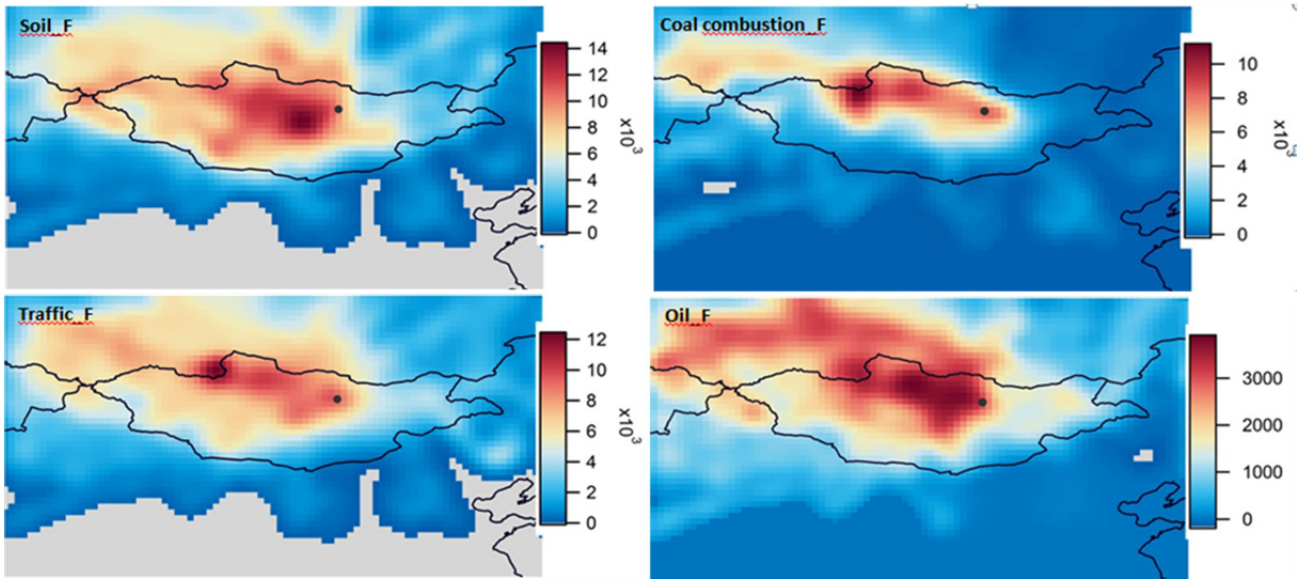

Fig. 8. CWT for the $PM_{2.5}$ source contributions showing potential source locations (concentrations in ng m^{-3}).

CONCLUSIONS

This study, which was conducted in Ulaanbaatar, Mongolia, provides insight into APM related pollution in the area.

PM samples were chemically analyzed with a secondary target commercial ED-XRF system, which was found to be highly suitable for rapid quantitative analysis. The obtained MDL values demonstrate that determining low concentrations of an element on a filter is possible.

Applying the PMF statistical technique to these PM samples, the elemental source fingerprints and contributions to the total mass were identified. The results of the study indicate that coal combustion for domestic heating is a primary source; additionally, the air quality in the area is significantly affected by the scattering of dust formed in heating ovens. Coal dust is produced in high amounts and, in many cases, discarded directly onto the soil. Thus, the resuspended dust is a combination of natural and anthropogenic emissions. This finding is confirmed by the source profiles and the temporal variation in the source contributions, which indicate that fly ash originating in

coal combustion is mixed with traffic emissions and resuspended soil. The following 4 sources were determined for both size fractions: soil, coal combustion, traffic and oil combustion. The respective contributions of these sources were 35%, 16%, 41% and 8% of the coarse fraction, whereas they were 31%, 27%, 31% and 11% of the fine fraction.

The mass contributions to the fine fraction show that combustion related sources dominate the cold season (October–March), whereas crustal matter sources dominate the warm season (April–September). In the coarse fraction, traffic (mixed with coal combustion) emissions dominate the cold season, whereas soil dominates the warm season.

Concentration-weighted trajectory analysis, which was applied to assess the influence of long-range transport on the sampling area, suggests that transported emissions primarily increase the contribution from heavy oil combustion.

Overall, this work highlights the importance of detailed air quality research in less studied areas. The differences in human habitat, environmental conditions and topography between the region we examined and other areas, such as Europe and North America, as well as other parts of Asia, create the opportunity to reevaluate the performance of well-known methods of environmental analysis.

ACKNOWLEDGEMENTS

This project was funded by Mongolian Foundation for Science and Technology and supported in part by the International Atomic Energy Agency (IAEA) through the Regional Cooperation Agreement Program "RAS/7/023."

Moreover, this work has been supported by the IAEA and the International Centre for Theoretical Physics and through an IAEA-ICTP Sandwich Training Educational Program fellowship C6/MON/15001 granted to Gerelmaa Gunchin.

REFERENCES

Calzolai, G., Chiari, M., Lucarelli, F., Mazzei, F., Nava, S., Prati, P., Valli, G. and Vecchi, R. (2008). PIXE and XRF analysis of particulate matter samples: An inter-laboratory comparison. *Nucl. Instrum. Methods Phys. Res., Sect. B* 266: 2401–2404.

Chandra, S., Kulshrestha, M.J. and Singh, R. (2014). Temporal variation and concentration weighted trajectory analysis of lead in PM_{10} aerosols at a site in Central Delhi, India. *Int. J. Earth Atmos*. 2014: 323040.

Cohen, D.D., Garton, D., Stelcer, E., Hawas, O., Wang, T., Poon, S., Kim, J., Choi, B.C., Oh, S.N., Shin, H.J., Ko, M.Y. and Uematsu, M. (2004). Multielemental analysis and characterization of fine aerosols at several key ACE-Asia sites. *J. Geophys. Res.* 109: D19S12.

Cohen, D.D., Stelcer, E., Atanacio, A. and Crawford, J. (2014). The application of IBA techniques to air pollution source fingerprinting and source apportionment. *Nucl. Instrum. Methods Phys. Res., Sect. B* 318: 113–118.

Davy, P.K., Gunchin, G., Markwitz, A., Trompetter, W.J., Barry, B.J., Shagjjamba, D. and Lodoysamba, S. (2011). Air particulate matter pollution in Ulaanbaatar, Mongolia: Determination of composition, source contributions and source locations. *Atmos. Pollut. Res*. 2: 126–137.

Diapouli, E., Manousakas, M., Vratolis, S., Vasilatou, V., Maggos, T., Saraga, D., Grigoratos, T., Argyropoulos, G., Voutsa, D., Samara, C. and Eleftheriadis, K. (2017). Evolution of air pollution source contributions over one decade, derived by PM_{10} and $PM_{2.5}$ source apportionment in two metropolitan urban areas in Greece. *Atmos. Environ.* 164: 416–430.

Eleftheriadis, K. and Colbeck, I. (2001). Coarse atmospheric aerosol: Size distributions of trace elements. *Atmos. Environ.* 35: 5321–5330.

Gunchin, G., Sereeter, L., Dagva, S., Tsenddavaa, A., Davy, P.K., Markwitz, A. and Trompetter, W.J. (2012). Air particulate matter pollution in Ulaanbaatar city Mongolia. *Int. J. PIXE* 22: 165–171.

Gutknecht, W., Flanagan, J., McWilliams, A., Jayanty, R.K.M., Kellogg, R., Rice, J., Duda, P. and Sarver, R.H. (2010). Harmonization of uncertainties of X-ray fluorescence data for $PM_{2.5}$ air filter analysis. *J. Air Waste Manage. Assoc*. 60: 184–194.

Guttikunda, S. (2007). *World bank consultant report*, Washington, DC, USA.

Hasenkopf, C.A., Veghte, D.P., Schill, G.P., Lodoysamba, S., Freedman, M.A. and Tolbert, M.A. (2016). Ice nucleation, shape, and composition of aerosol particles in one of the most polluted cities in the world: Ulaanbaatar, Mongolia. *Atmos. Environ.* 139: 222–229.

Lide, D.R. (1992). *CRC handbook of chemistry and physics*, CRC Press. Boca Raton, Florida.

Maenhaut, W., Francois, F. and Cafmeyer, J. (1993). The GENT stacked filter unit sampler for collection of atmospheric aerosols in two size fractions. Report No. NAHRES-19, International Atomic Energy Agency, Vienna, pp. 249–263.

Manousakas, M., Diapouli, E., Papaefthymiou, H., Migliori, A., Karydas, A.G., Padilla-Alvarez, R., Bogovac, M., Kaiser, R.B., Jaksic, M., Bogdanovic-Radovic, I. and Eleftheriadis, K. (2015). Source apportionment by PMF on elemental concentrations obtained by PIXE analysis of PM_{10} samples collected at the vicinity of lignite power plants and mines in Megalopolis, Greece. *Nucl. Instrum. Methods Phys. Res., Sect. B* 349: 114–124.

Manousakas, M., Papaefthymiou, H., Diapouli, E., Migliori, A., Karydas, A.G., Bogdanovic-Radovic, I. and Eleftheriadis, K. (2017). Assessment of $PM_{2.5}$ sources and their corresponding level of uncertainty in a coastal urban area using EPA PMF 5.0 enhanced diagnostics. *Sci. Total Environ*. 574: 155–164.

Ostro, B., Tobias, A., Karanasiou, A., Samoli, E., Querol, X., Rodopoulou, S., Basagaña, X., Eleftheriadis, K., Diapouli, E., Vratolis, S., Jacquemin, B., Katsouyanni, K., Sunyer, J., Forastiere, F. and Stafoggia, M. (2015). The risks of acute exposure to black carbon in Southern Europe: Results from the MED-PARTICLES project. *Occup. Environ Med.* 72: 123–129.

Paatero, P. (1997). Least squares formulation of robust non-negative factor analysis. *Chemom. Intell. Lab. Syst.* 37: 23–35.

Paatero, P. and Hopke, P.K. (2003). Discarding or downweighting high-noise variables in factor analytic models. *Anal. Chim. Acta* 490: 277–289.

Paatero, P., Hopke, P.K., Hoppenstock, J. and Eberly, S.I. (2003). Advanced Factor Analysis of Spatial Distributions of $PM_{2.5}$ in the Eastern United States. *Environ. Sci. Technol.* 37: 2460–2476.

Petit, J.E., Favez, O., Albinet, A. and Canonaco, F. (2016). A user friendly tool for comprehensive evaluation of the geographical origins of atmospheric pollution: Wind and trajectory analyses. *Environ. Modell. Software* 88: 183–187.

Prost, J., Zinkl, A., Ingerle, D., Wobrauschek, P. and Streli, C. (2018). Evaluation of a sample preparation procedure for total-reflection X-ray fluorescence analysis of directly collected airborne particulate matter samples. *Spectrochim. Acta, Part B* 147: 13–20.

Reff, A., Eberly, S.I. and Bhave, P.V. (2007). Receptor modeling of ambient particulate matter data using positive matrix factorization: Review of existing methods. *J. Air Waste Manage. Assoc*. 57: 146–154.

Santoso, M., Hopke, P.K., Hidayat, A. and Diah Dwiana, L. (2008). Sources identification of the atmospheric aerosol at urban and suburban sites in Indonesia by positive matrix factorization. *Sci. Total Environ*. 397: 229–237.

Sarigiannis, D.A., Handakas, E.J., Kermenidou, M., Zarkadas, I., Gotti, A., Charisiadis, P., Makris, K., Manousakas, M., Eleftheriadis, K. and Karakitsios, S.P. (2017). Monitoring of air pollution levels related to Charilaos Trikoupis Bridge. *Sci. Total Environ.* 609: 1451–1463.

Shaltout, A.A., Boman, J. and Alsulimane, M.E. (2017). Identification of elemental composition of $PM_{2.5}$ collected in Makkah, Saudi Arabia, using EDXRF. *X-Ray Spectrom.* 46: 151–163.

Shaltout, A.A., Hassan, S.K., Karydas, A.G., Zaki, Z.I., Mostafa, N.Y., Kregsamer, P., Wobrauschek, P. and Streli, C. (2018). Comparative elemental analysis of fine particulate matter ($PM_{2.5}$) from industrial and residential areas in Greater Cairo-Egypt by means of a multi-secondary target energy dispersive X-ray fluorescence spectrometer. *Spectrochim. Acta, Part B* 145: 29–35.

Ulaanbaatar City Governor'S Implementation Agency (2016). *Ulaanbaatar statistical report.* Department of Statistics, Ulaanbaatar City Governor's Implementation Agency, Mongolia.

Wang, Y.Q., Zhang, X.Y. and Draxler, R.R. (2009). TrajStat: GIS-based software that uses various trajectory statistical analysis methods to identify potential sources from long-term air pollution measurement data. *Environ. Modell. Software* 24: 938–939.

World Bank (2011). *World bank report. Ulaanbaatar, Mongolia*. World Bank, Washington, DC, USA.

World Health Organization (WHO) (2005). Air quality guidelines. Global update 2005. Particulate matter, ozone, nitrogen dioxide and sulfur dioxide. WHO Press, World Health Organization, Switzerland.

Received for review, September 25, 2018
Revised, January 8, 2019
Accepted, January 8, 2019